A TABLE OF GENUS TWO HANDLEBODY-KNOTS WITH SEVEN CROSSINGS

GIOVANNI BELLETTINI, GIOVANNI PAOLINI, MAURIZIO PAOLINI, AND YI-SHENG WANG

ABSTRACT. We enumerate all genus two handlebody-knots with seven crossings, up to mirror image, extending the Ishii-Kishimoto-Moriuchi-Suzuki table.

1. Introduction

A genus g handlebody-knot is an embedded handlebody V of genus g in the oriented 3-sphere \mathbb{S}^3 , and a spatial graph is an embedded finite graph Γ in \mathbb{S}^3 . A spine of a handlebody-knot is a spatial graph, and a regular neighborhood of a spatial graph is a handlebody-knot. While every spatial graph has a unique regular neighborhood, up to isotopy, a handlebody-knot can have infinitely many different spines. Two handlebody-knots V, V' (resp. spatial graphs Γ, Γ') are equivalent if there is an orientation-preserving self-homeomorphism of \mathbb{S}^3 sending V to V' (resp. sending Γ to Γ'); if the condition "orientation-preserving" is dropped, we say they are equivalent, up to mirror image. The crossing number of a handlebody-knot V is the minimum of the crossing numbers of all its spines. A handlebody-knot V is irreducible if there exists no 2-sphere in \mathbb{S}^3 meeting V at an essential disk of V.

Ishii-Kishimoto-Moriuchi-Suzuki [8, Table 1] enumerates, up to mirror image, all irreducible genus two handlebody-knots, up to six crossings. Our main result extends their table to seven crossing genus two handlebody-knots.

Theorem 1.1. Table 1 enumerates all irreducible genus two handlebody-knots with seven crossings, up to mirror image.

The construction of Table 1 allows us to obtain a table of reducible handlebody-knots, extending [8, Table 4].

Theorem 1.2. Table 2 enumerates all reducible genus two handlebody-knots with seven crossings, up to mirror image.

The paper is structured so that the completeness of the two tables is given in Section 3, while in Sections 4 and 6, we prove that there are no duplications in Tables 1, 2. Section 5 explains how the irreducibility of handlebody-knots in Table 1 is obtained.

2. Preliminaries

2.1. **Diagrams.** Given a spatial graph Γ and $p \in \mathbb{S}^3 - \Gamma$, then we say a projection $\pi : \mathbb{S}^3 - \{p\} \simeq \mathbb{R}^3 \to \mathbb{R}^2$ is regular with respect to Γ if π is in general position [20] (see [6, Sectino 4.4]). In particular, the image $\pi(\Gamma)$ is a plane graph with vertices the union of double points of π and vertices of Γ .

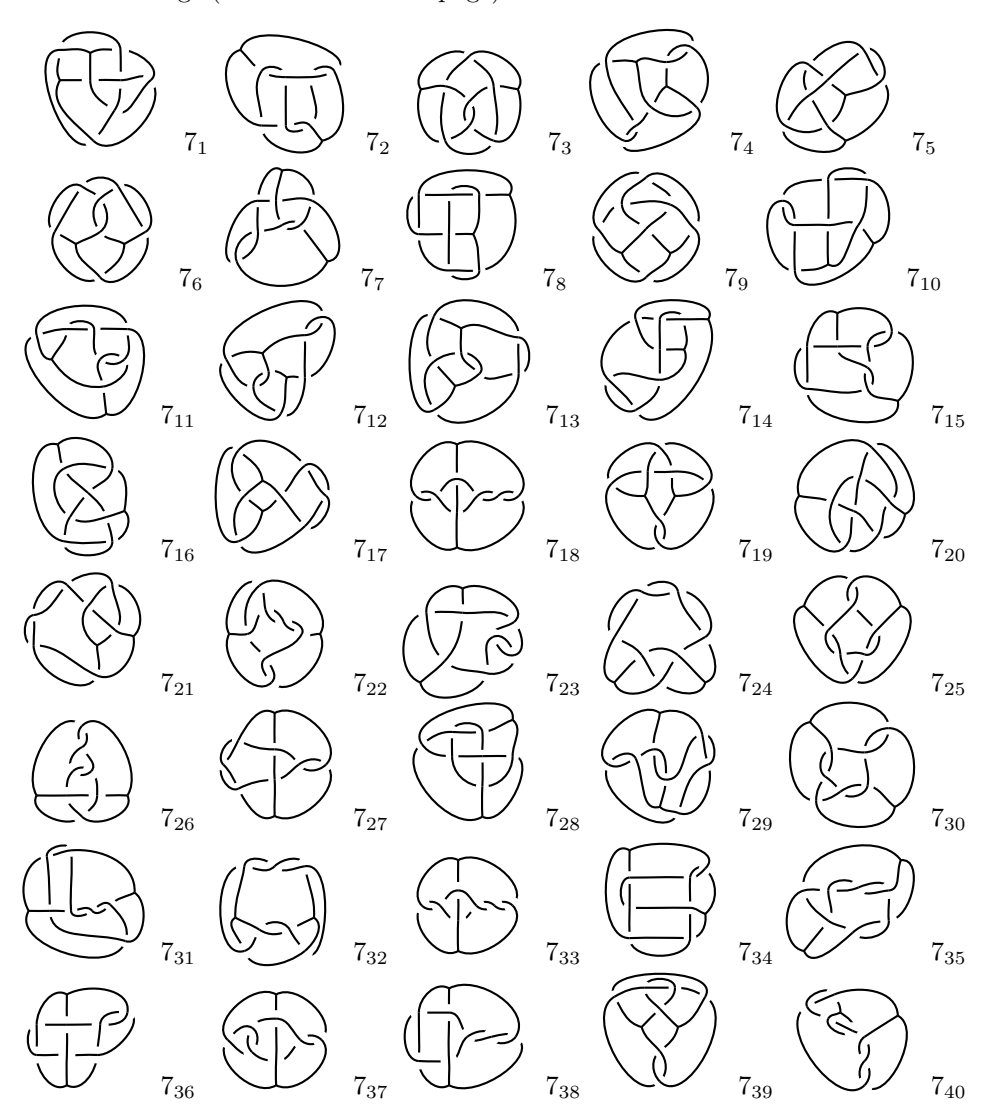
Given a regular projection π with respect to Γ , a diagram of Γ is given by replacing each double point in $\pi(\Gamma)$ with a crossing, where the broken arc corresponds to

Date: November 18, 2025.

²⁰²⁰ Mathematics Subject Classification. 57K12, 57M15, 05C30.

Key words and phrases. handlebody-knot table, spatial graphs.

TABLE 1. Irreducible genus two handlebody knots with seven crossings (continued on next page).



the edge of Γ underneath the edge the unbroken arc corresponds to in $\mathbb{R}^3 \simeq \mathbb{S}^3 - \{p\}$; see Fig. 2.1a. A diagram of a handlebody-knot V is a diagram of one of its spines. The plane graph $\pi(\Gamma)$ is called the underlying graph of the diagram.

The crossing number of a diagram of a spatial graph Γ (resp. handlebody-knot V) is the number of the crossings the diagram has. The crossing number $c(\Gamma)$ of Γ (resp. c(V) or V) is the minimum of the crossing numbers over all diagrams of Γ (resp. V). A diagram of Γ (resp. V) that attains the crossing number of Γ (resp. V) is called a minimal diagram. A minimal diagram of Γ is in general not unique.

Given a diagram D of a spine Γ of a handlebody-knot V, observe that if $v \in D$ is a vertex of valence greater than 3 and $\mathcal{N}(v) \subset \mathbb{R}^2$ is a regular neighborhood of v with $D_v := D \cap \mathcal{N}(v)$ a deformation retract of $\mathcal{N}(v)$, then we can replace D_v with a new graph \tilde{D}_v where $\tilde{D}_v \cap \partial \mathcal{N}(v) = D_v \cap \partial \mathcal{N}(v)$ and all vertices of \tilde{D}_v in the interior of $\mathcal{N}(V)$ are trivalent; see Fig. 2.1b. In particular, every handlebody-knot has a minimal diagram which is a diagram of a trivalent spine—namely, all vertices are trivalent.

Table 1. (continued)

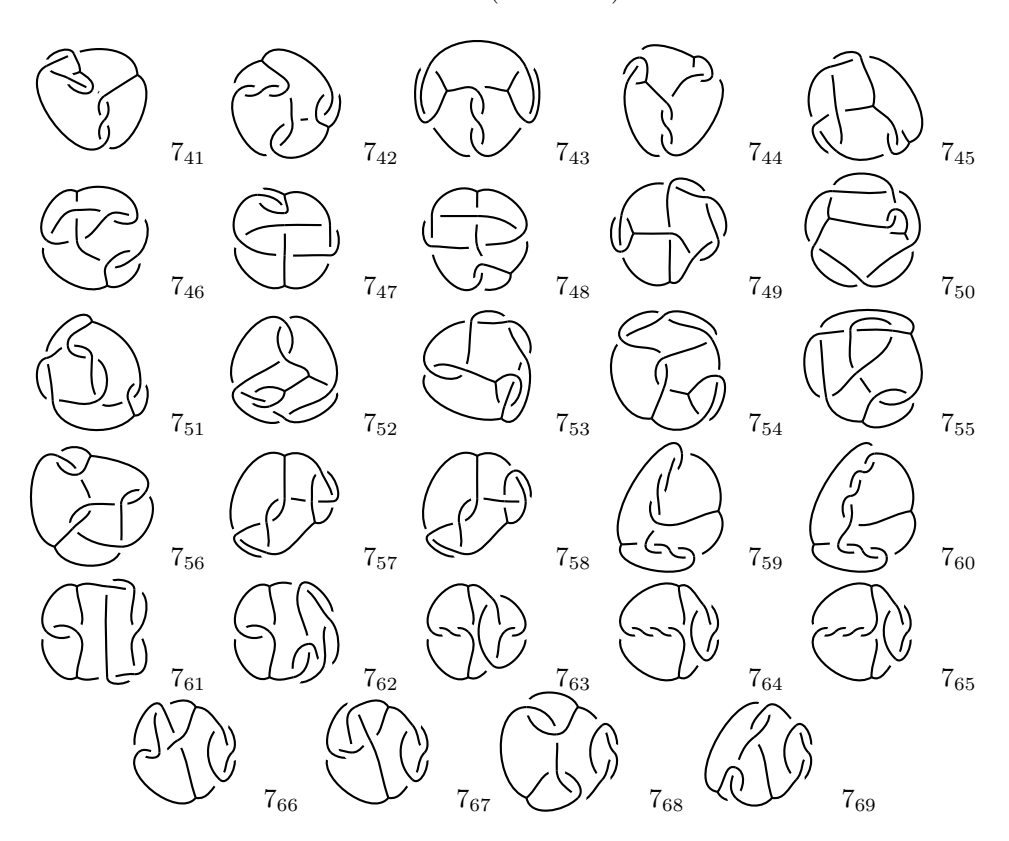
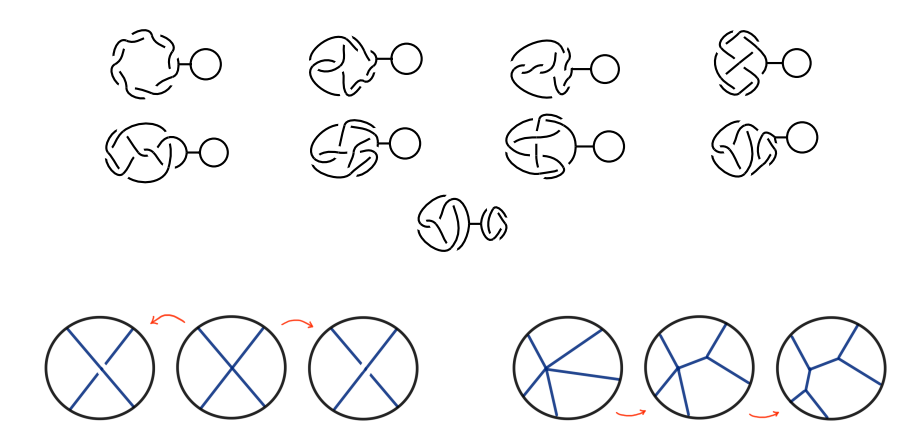


Table 2. Reducible handlebody knots with seven crossings.



(a) Turning 4-valent vertices into crossings.

(b) Turning into trivalent vertices.

FIGURE 2.1

A trivalent spine of a genus g handlebody-knot has 2g-2 trivalent vertices. Therefore, a trivalent spine of a genus two handlebody-knot is either a spatial theta graph or a spatial handcuff graph. For the sake of simplicity, hereinafter, a minimal diagram always refers to a minimal diagram of a trivalent spatial graph or a trivalent spine of a handlbody-knot.

Recall that the *edge-connectivity* of a graph is the minimum number of edges whose deletion disconnects the graph. A graph is e-connected if it has edge-connectivity greater than or equal to e. A diagram of a spatial graph is said to have *connectivity* e (resp. to be e-connected) if its underlying graph has edge-connectivity e (resp. is e-connected).

To study handlebody-knots in terms of their diagrams, we recall that *generalized Reidemeister moves* are the local changes depicted in Figs. 2.2 and 2.3 and an *IH-move* is the local change in Fig. 2.4.

Theorem 2.1 ([7, Corollary 2]). Two handlebody-knots are equivalent if and only if their diagrams are related by a finite sequence of generalized Reidemeister moves and IH-moves.

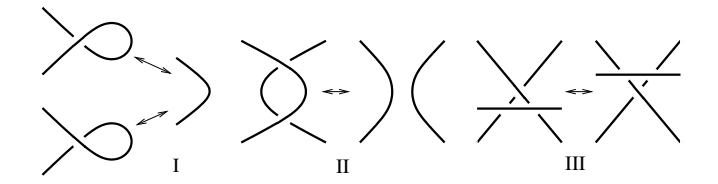


FIGURE 2.2. Classical Reidemeister moves of type I, II, III.

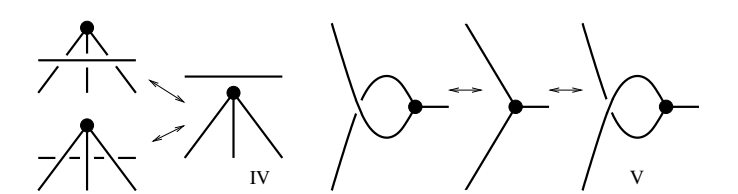


FIGURE 2.3. Reidemeister moves IV and V involving a trivalent vertex.

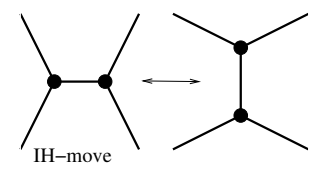


FIGURE 2.4. IH-move.

3. Completeness

Hereinafter, for the sake of simplicity, unless otherwise specified, by a handlebody-knot, we understand a genus two handlebody-knot. To enumerate all seven crossing handlebody-knots, our approach is to divide minimal diagrams into three classes:

- (1) 3-connected minimal diagrams;
- (2) Minimal diagrams with connectivity 2;
- (3) Minimal diagrams with connectivity 1.

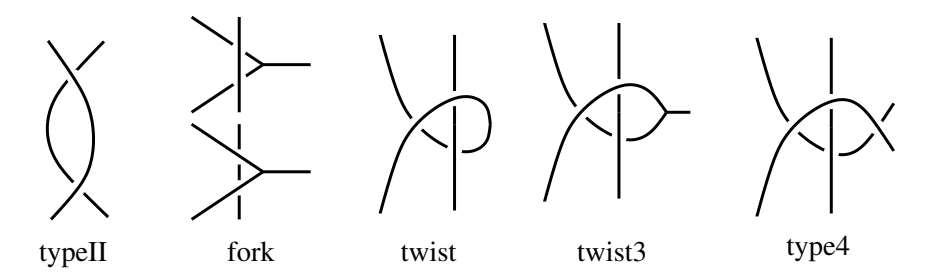


FIGURE 3.1. Crossing-reducing moves.

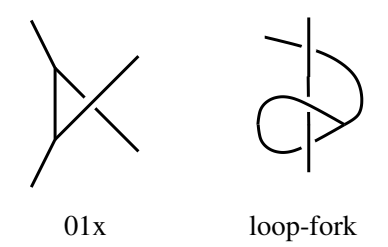


FIGURE 3.2. More crossing-reducing moves. "01x" is an IH-move followed by a Move V; "loop-fork" is given by twisting the loop and then a fork in Fig. 3.1.

- 3.1. 3-connected diagrams. Our goal here is to find all seven crossing handlebody-knots that have a 3-connected minimal diagram. To do so, we first enumerate all 3-connected plane graphs with two trivalent vertices and seven quadrivalent vertices, and then substitute each quadrivalent vertex with a crossing. 1 The first part is done by a code devised by the second author, and it results in 908 such plane graphs, up to mirror image. Since, for each quadrivalent vertex, there are two possible choices of crossings (see Fig. 2.1a), these 908 plane graphs produce an unmanageable number, $908 \cdot 2^6$, of diagrams, up to mirror image. To reduce the number of diagrams, a software developed by the third author is implemented to drop diagrams that
 - represent a handlebody-link with more than one component, or
 - is recognized to be nonminimal via moves in Figs. 3.1 and 3.2.

In addition, one choice is selected for any pair of over/under crossings

• that results in embeddings having a portion depicted in Fig. ??.

Consequently, we obtain a refined set \mathcal{D}_3 of 932 diagrams, where, for every seven crossing handlebody-knot V with a 3-connected minimal diagram, there is a minimal diagram in \mathcal{D}_3 representing V.

3.2. **Diagrams with connectivity** 2. The aim here is to find all seven crossing handlebody-knots that have a minimal diagram with connectivity 2 and no minimal diagram with connectivity 1.

 $^{^{1}}$ Note that the Whitney theorem [19] is not applicable here since a 3-connected graph may not be 3-vertex-connected.

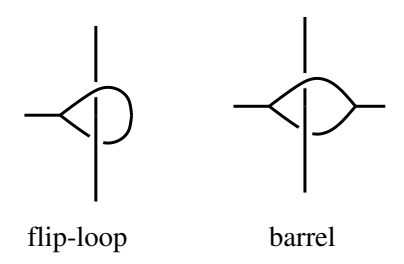


FIGURE 3.3. Loop flipping moves.

2-sum of diagrams and spatial graphs. A 2-sum of two spatial graphs Γ_1, Γ_2 is constructed as follows [11]: For each i=1,2, we first orient every arc in Γ_i , and secondly, consider a 3-ball B_i with $B_i \cap \Gamma_i$ a subarc of an edge e_i of Γ_i ; denote by a_i the point in $e_i \cap \partial B_i$ where e_i is going out of B_i and by b_i the other point in $\partial B_i \cap e_i$. Then the order-2 vertex connected sum, abbreviated to 2-sum, is the spatial graph given by gluing the exteriors $E(B_1)$ and $E(B_2)$ with an orientation-reversing homeomorphism $h: \partial E(B_1) \to \partial E(B_2)$ with $h(a_1) = b_2$, $h(b_1) = a_2$. The spatial graphs Γ_1 , Γ_2 are called summands of the 2-sum.

Since a 2-sum depends on the oriented trivial ball-arc pairs chosen, it is not unique, and $\Gamma_1 \# \Gamma_2$ denotes the set of all possible 2-sums of Γ_1 or its mirror image and Γ_2 or its mirror image.

Given a diagram D of a handlebody-knot V, a prime factor $N \subset \mathbb{R}^2$ of D is a disk N with ∂N meeting D at two points a,b such that $N \cap D$ together with an arc outside N is a diagram of a prime knot K, called the *induced prime knot*. A system \mathcal{N} of prime factors is a set of mutually disjoint prime factors, and it is maximal if it is not a proper subset of another system of prime factors.

Given a system $\mathcal{N} = \{N_1, \dots, N_k\}$ of prime factors, let α_i be an arc in N_i with $\partial \alpha_i = D \cap \partial N_i$, then $(D - (N_1 \cup \dots \cup N_k)) \cup (\alpha_1 \cup \dots \cup \alpha_k)$ is a diagram D_0 of a spatial handcuff or theta graph Γ_0 ; D_0 and Γ_0 are called the *base diagram* and *base graph*, respectively.

Suppose D is minimal with 7 crossings and connectivity 2. Then D admits a non-empty maximal system $\mathcal{N} = \{N_1, \dots, N_k\}$ of prime factors, and the base graph D_0 is 3-connected and minimal. Since D has only 7 crossings and a non-trivial knot has at least 3 crossings, we have k = 2, and

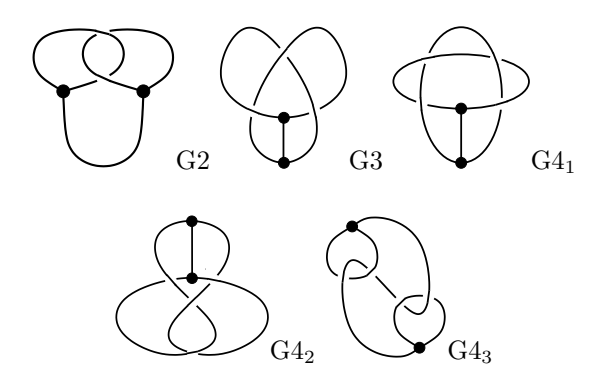
$$\Gamma \in (\Gamma_0 \# K_1) \# K_2$$

where K_1, K_2 are the prime knots induced by N_1, N_2 , respectively. The base graph Γ_0 cannot be a trivial spatial handcuff since V admits no minimal diagram with connectivity 1. If Γ_0 is a trivial spatial θ -graph, then, since $k \leq 2$, there is an edge in D joining the two trivalent vertices. Thus an IH-move along that edge turns D into a minimal diagram with connectivity 1, contradicting our assumption. As a result, Γ_0 is non-trivial, and hence D_0 has at least two crossings, so k=1, and K_1 is prime and has at most five crossings, and Γ_0 has at most four crossings.

Since prime knots up to five crossings are all invertible, the set $\Gamma_0 \# K_1$ contains at most six elements, depending on the arc in Γ_0 where the 2-sum is performed and the chirality of K_1 . Note that handlebody-knots so produced might not have seven crossings.

To determine Γ_0 , we note that, since D_0 is 3-connected, it suffices to enumerate all spatial graphs that have a 3-connected minimal diagram, up to four crossings. This is done by the code developed by the second author, which allows us to find all

Table 3. Spatial graphs up to four crossings.



3-connected plane graphs with two trivalent vertices and up to four quadrivalent vertices. Such spatial graphs are enumerated in Table 3 (see [4, Table 4] and [11, 12]). Denote by $\mathrm{Kn_m}$ the prime knot $\mathrm{n_m}$ in the knot table. Then, since Γ_0 is in Table 3, seven crossing handlebody-knots V that have a minimal diagram with connectivity 2 but no minimal diagram with connectivity 1 can be enumerated as follows.

- $G2 \# K3_1$: the handlebody-knot 5_4 of [8, Table 1];
- G3 # K3₁: the handlebody-knots 6_{14} and 6_{15} of [8, Table 1].
- $G2 \# K4_1$: the handlebody-knot 6_{16} of [8, Table 1];
- $G2 \# K5_1$: the handlebody-knot 7_{61} of Table 1;
- $G2 \# K5_2$: the handlebody-knot 7_{62} of Table 1;
- $G3 \# K4_1$: the handlebody-knot 7_{63} of Table 1;
- $G4_1 \# K3_1$: the handlebody-knots 7_{64} and 7_{65} of Table 1
- $\bullet~ \mathrm{G4}_2 \, \# \, \mathrm{K3}_1 \colon$ the handlebody-knots 7_{66} and 7_{67} of Table 1.
- $G4_3 \# K3_1$: the handlebody-knots 7_{68} and 7_{69} of Table 1.

Each handlebody-knot above admits a canonical diagram with a single prime factor associated to a minimal diagram of Kn_m ; see Table 1. the set of the diagrams are denoted by \mathcal{D}_2 .

3.3. **Diagrams with connectivity** 1. The aim here is to find all seven crossing handlebody-knots that have a minimal diagram with connectivity 1.

1-sum of handlebody-knots. Let V_1, V_2 be two handlebody-knots of genus g_1, g_2 , respectively. Then the 1-sum $V_1 - V_2$ is constructed as follows: For each i = 1, 2, choose a 3-ball B_i such that $D_i := V_i \cap B_i = \partial V_i \cap \partial B_i$ is a disk. Let $h: \partial E(B_1) \to \partial E(B_2)$ be an orientation-reversing homeomorphism with $h(D_1) = D_2$. Then $V_1 - V_2$ is the genus $g_1 + g_2$ handlebody-knot obtained by gluing $D_1 \subset V_1$ to $D_2 \subset V_2$ via h in the 3-sphere $E(B_1) \cup_h E(B_2)$; see Fig. 3.4.

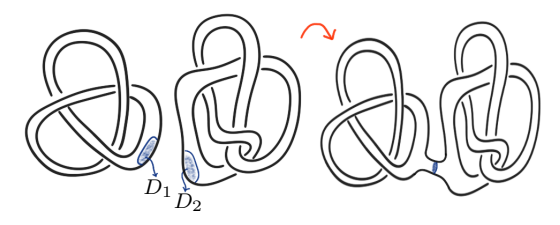


FIGURE 3.4. One sum of $K3_1$ and $K4_1$.

Enumeration. Suppose the handlebody-knot V has a minimal diagram D with connectivity 1, and let $e \in D$ be the edge cutting which disconnects D. Then $D-\{e\}$ consists of two components D_1, D_2 . Let V_1, V_2 be the genus one handlebody-knots represented by D_1, D_2 . Then D is a diagram of $V_1 - V_2$. Therefore, to enumerate handlebody-knots with a minimal diagram of connectivity 1, it suffices to consider all one sums $V_1 - V_2$ with $V_1 \cdot V_2$ of genus one and $c(V_1) + c(V_2) = 7$. Since a genus one handlebody-knot is equivalent to a knot, we use the same notation Kn_m to denote the genus one handlebody-knot corresponding to the prime knot Kn_m , and let $K0_1$ be the trivial genus one handlebody-knot.

```
• K7_1 - K0_1;
```

- $K7_2 K0_1$;
- $K7_3 K0_1$;
- K7₄ -- K0₁;
- K7₅ -- K0₁;
- K7₆ -- K0₁;
- K7₇ -- K0₁;
- K4₁ -- K3₁;
- $(K4_1 \# K3_1) K0_1$.

For each handlebody-knot above, there is a canonical diagram given by minimal diagrams of Kn_m as shown in Table 2; the set of diagrams is denoted by \mathcal{D}_1 .

3.4. Conclusion. Let $\mathcal{D} = \mathcal{D}_1 \cup \mathcal{D}_2 \cup \mathcal{D}_3$.

Theorem 3.1 (Completeness). For every seven crossing handlebody-knot V, there is a minimal diagram in \mathcal{D} representing V.

Proof. If V has no minimal diagram with connectivity 1, then it has a minimal diagram constructed in Sections 3.1 and 3.2. If V has a minimal diagram with connectivity 1, then it has one constructed in Section 3.3.

Remark 3.1. In general, it is not known whether the minimal diagram of a 1-sum always has connectivity 1. Similarly, it is unclear whether a minimal diagram of a handlebody-knot having a spine that is a 2-sum always has connectivity 2.

Remark 3.2. Recall that a spatial graph Γ is *prime* if, for any 3-ball B with ∂B meeting Γ transversally at less than or equal to 3 points, the intersection $B \cap \Gamma$ is contained in a proper disk in B; see [12], [11]. In particular, if Γ has a diagram with connectivity less than or equal to 3, then Γ cannot be prime.

Tables of prime spatial handcuff graphs and θ -graphs, up to seven crossings, are given in Moriuchi [12], [11]. There are however at least 20 handlebody-knots in Table 1 that do not have any 3-connected minimal diagram. Also, two inequivalent seven crossing spatial graphs may represent the same handlebody-knots; for instance, up to mirror image, the spatial θ -graphs 7_{21} , 7_{60} in [11] and handcuff graph 7_{21} in [12] all represent the same handlebody-knot 7_{36} in Table 1; similarly, the spatial θ -graphs 7_{18} , 7_{48} , 7_{58} in [11] all represent the handlebody-knot 7_{52} in Table 1, and the spatial handcuff graph 7_{17} in [12] and θ -graph 7_{16} in [13] both represent the handlebody-knot 7_{32} in Table 1.

A minimal diagram of a spatial graph might not be minimal as a diagram of a handlebody-knot. For instance, from spatial θ -graphs 7_{25} to 7_{39} in [11] are all non-minimal as diagrams of handlebody-knots. A detailed correspondence between diagrams in [12], [11] to the seven crossing handlebody-knots can be found in [16].

4. NO DUPLICATES IN THE TABLE

Our goal is to classify diagrams in \mathcal{D} into several classes, each of which contains only diagrams that represent the same handlebody-knot, up to equivalence and

mirror image. Given the sheer size of \mathcal{D} , we adopt a dynamic approach to classify diagrams in \mathcal{D} .

4.1. A dynamic approach. The dynamic approach can be pictured as a growing rooted tree. The end result is a big rooted tree \mathcal{T} , which is a dynamic data structure with data attached to each leaf. Specifically, each leaf of \mathcal{T} contains diagrams that represent one or two equivalence classes of handlebody-knots, up to mirror image.

The tree \mathcal{T} is grown from the degenerate tree with a single vertex, the root, containing all diagrams in \mathcal{D} . At start, we apply some weak but computationally efficient invariant t_1 to handlebody-knots represented by diagrams in the root. The diagrams in \mathcal{D} are then divided into classes so that each class contains only diagrams with the same t_1 -invariant. We associate each class with a new leaf connecting to root with an edge, and thus the initial degenerate tree grows into a star. Next, for each leave v of the star, we apply a slightly stronger invariant t_2 , specifically tailored to the leaf v. Thus t_2 divides the diagrams in the leaf v into even smaller classes based on their t_2 -invariants. In the same way, we associate each class with a new leaf connecting to v with an edge; note that v is no longer a leaf at this stage. The process repeats itself for each leaf, and whenever we arrive at a stage where the leaf contains only a handful of diagrams or no computationally affordable invariant can distinguish the handlebody-knots the diagrams therein represent, we tag the leaf as final. The big tree \mathcal{T} is then the resulting tree, where every leaf is tagged as final; see the web page [16] for a snapshot.

The invariants used here are the Kitano-Suzuki invariants. Given a handlebody-knot V, let G be a finite group, then the Kitano-Suzuki G-invariant ks_G is the number of conjugate classes of homomorphisms from the fundamental group of the exterior E(V) of V to G. When the order of G is small, the computation load of ks_G is rather light, but it grows exponentially as the order of G gets larger. The computational complexity is also highly sensitive to the number of generators in the used presentation of the fundamental group. The finite groups used in our computation are

- $SL_2(\mathbb{Z}_p)$ with prime p,
- The symmetric group S_n , $n \in \mathbb{N}$,
- The alternating group A_n , $n \in \mathbb{N}$.

In the process of building the tree \mathcal{T} , we start with G of a smaller size and move on to larger ones.

The invariant ks_G depends only on the exterior of a handlebody-knot, so it cannot differentiate inequivalent handlebody-knots with homeomorphic exteriors; such handlebody-knots, however, abound [14], [10], [1]. A stronger invariant, the *G-image* invariant introduced in [1] is thus used. The *G-image* invariant is constructed as follows: Consider the homomorphisms

$$\iota_{1*}: \pi_1(\partial V) \to \pi_1(V), \quad \iota_{2*}: \pi_1(\partial V) \to \pi_1(E(V))$$

induced by the inclusions $\iota_1:\partial V\to V$ and $\iota_2:\partial V\to E(V)$. Then a surjective homomorphism from $\pi_1(E(V))$ to a finite group G is said to be *proper* if it becomes non-surjective after precomposed with i_{2*} . The G-image is then given by the set of the images of the subgroup $i_{2*}(\operatorname{Ker}(i_{1*}))$ in G under proper homomorphisms.

The computation of the invariants listed above are automatized by a software developed by the third author. Once we obtain the tree \mathcal{T} , we check semi-manually, via Theorem 2.1, the equivalence of diagrams in each leaf. Most of them are shown to contain only one equivalence class of handlebody-knots. As an exception we have the five pairs: $(5_1, 7_{39})$, $(7_{40}, 7_{41})$, $(7_{43}, 7_{44})$, $(7_{59}, 7_{60})$, and $(6_{12}, 7_{39})$, the two handlebody-knots in each pair have the same values of all computed invariants, and therefore are in the same leaf, where $5_1, 6_{12}$ are taken from the table [8]. To

distinguish them, other methods are therefore required. The inequivalence between members in the pairs $(7_{59}, 7_{60})$ and $(6_{12}, 7_{39})$ are shown in [5], while Section 6 deals with the other three pairs $(7_{40}, 7_{41})$, $(5_1, 7_{52})$, and $(7_{43}, 7_{44})$. The end result is then the union of Tables 1 and 2. ²

5. Irreducibility

To divide the handlebody-knots into Tables 1 and 2, we need to determine their irreducibility.

Recall that the rank of a handlebody-knot V is the minimal number of generators needed to generate the fundamental group $\pi_1(E(V))$. Most handlebody-knots in Table 1 are of rank 3. For a few of them, such as 7_{68} , 7_{69} , we only know their ranks do not exceed 4. The irreducibility of handlebody-knots in Table 1 is detected by the following criteria derived from [2, Theorems 1.1, 1.2].

Theorem 5.1. Let V be a handlebody-knot. Suppose either

- (i) the rank of V is less than or equal to 3, and its ks_{A_5} -invariant is not congruent to 17 modulo 60, or
- (ii) the rank of V is less than or equal to 4, and its ks_{A_4} -invariant is not congruent to 10 modulo 12.

Then V is irreducible.

6. Hard pairs

Here we prove the inequivalence of the two handlebody-knots in each of the pairs: $(5_1, 7_{52})$, $(7_{40}, 7_{41})$, $(7_{43}, 7_{44})$. Recall from [9], a 3-decomposing sphere of a handlebody-knot V is a 2-sphere S meeting V at three disks such that $S \cap E(V)$ is incompressible in E(V). If in addition, the three disks in $S \cap V$ are parallel in V. Then S is called a P_3 -sphere of V; see [3]. A maximal P_3 -system S is a set $\{S_1, \ldots, S_n\}$ of mutually disjoint P_3 -spheres such that the intersections $S_i \cap E(V)$, $i = 1, \ldots, n$, are mutually non-parallel in E(V). By [3, Theorem 1.1], if V admits two maximal P_3 -systems S, S', then there exists a self-homeomorphism of (\mathbb{S}^3, V) sending S to S'.

Theorem 6.1. 743, 744 are inequivalent.

²The authors are informed that the pairs $(7_{40}, 7_{41})$, $(7_{43}, 7_{44})$, $(7_{59}, 7_{60})$ can be differentiated by quandle invariants, and Ishii-Kishimoto have independently obtained a similar table with 69 entries, where they find 3 hard pairs.

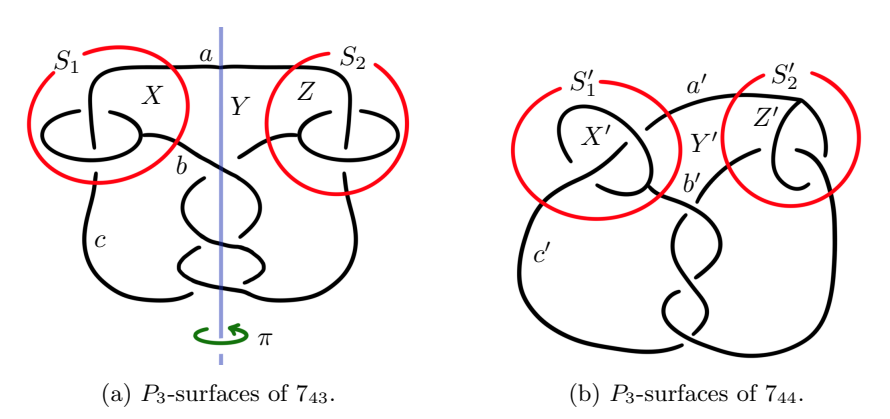


FIGURE 6.1

Proof. Denote by V (resp. by V') the handlebody-knot 7_{43} (resp. 7_{44}), and note that the spheres S_1, S_2 (resp. S'_1, S'_2) in Fig. 6.1a (resp. Fig. 6.1b) both are P_3 -spheres. Observe that the union $S_1 \cup S_2$ (resp. $S'_1 \cup S'_2$) cuts \mathbb{S}^3 into three components X, Y, Z (resp. X', Y', Z') as shown in Fig. 6.1a, (resp. Fig. 6.1b).

Consider the unions $E(X) \cup V$, $E(Y) \cup V$, and $E(Z) \cup V$ (resp. $E(X') \cup V'$, $E(Y') \cup V'$, and $E(Z') \cup V'$), and observe that they are all genus two handlebodies. Additionally, the disks in the intersection $V \cap (S_1 \cup S_2)$ (resp. $V' \cap (S'_1 \cup S'_2)$) induce a spine for each of them, and hence induce three spatial graphs $\Gamma_X, \Gamma_Y, \Gamma_Z$ (resp. $\Gamma_{X'}, \Gamma_{Y'}, \Gamma_{Z'}$).

The spatial graphs Γ_X , Γ_Z , $\Gamma_{X'}$, $\Gamma_{Z'}$ are the spatial handcuff graph G2 in Table 3, namely 2_1 in [12], while Γ_Y , $\Gamma_{Y'}$ are the mirror image of G3 in Table 3, namely 3_1 in [11], so they are all prime. This implies that $\{S_1, S_2\}$ (resp. $\{S_1', S_2'\}$) is a maximal P_3 -system.

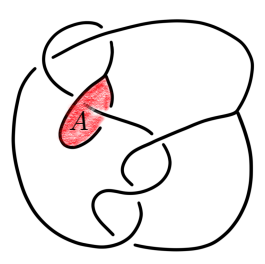
Label the arcs in Γ_Y and $\Gamma_{Y'}$ by a,b,c and a',b',c', respectively; see Figs. 6.1a, 6.1b. Then, by the uniqueness of the maximal P_3 -system [3, Theorem 1.1] and the fact that there is a self-homeomorphism of (\mathbb{S}^3,V) swapping S_1,S_2 (see Fig. 6.1a), there is a self-homeomorphism f of (\mathbb{S}^3,V) with $f(S_i)=S_i',\ i=1,2$. In particular, f induces an equivalence g from Γ_Y to $\Gamma_{Y'}$ with $g(a)=c',\ g(b)=b',\$ and g(c)=a'. This contradicts the fact that the constituent knot $b\cup c$ of Γ_Y is a trefoil knot, whereas the constituent knot $b'\cup a'$ of $\Gamma_{Y'}$ is trivial; see G3 in Table 3.

Theorem 6.2. 7_{40} and 7_{41} are inequivalent.

Proof. Denote by V, V' the handlebody-knots $7_{40}, 7_{41}$, respectively, and observe that E(V) (resp. E(V')) admits an essential annulus A (resp. A') as shown in Fig. 6.2a (resp. 6.2b). Let $\mathcal{N}(A)$ (resp. $\mathcal{N}(A')$) be a regular neighborhood of A in E(V) (resp. A' in E(V')). Then the union $V \cup \mathcal{N}(A)$ (resp. $V' \cup \mathcal{N}(A')$) in \mathbb{S}^3 is the handlebody-knot 5_1 , denoted by V_0 ; see Fig. 6.2c. By [18, Theorem 1.4], the exterior $E(V_0)$ admits a unique essential annulus A_0 .

Claim: A (resp. A') is the unique annulus in E(V) (resp. E(V')). Denote by l_1, l_2 the components of ∂A . Suppose E(V) admits an essential annulus non-isotopic to A. By the JSJ-decomposition of E(V), there exists an essential annulus $A^* \subset E(V)$ disjoint from A. Thus A^* can be regarded as an annulus in the exterior $E(V_0)$, and the incompressibility of $A^* \subset E(V)$ implies that it is incompressible in $E(V_0)$.

Let A_+, A_- be the components in the frontier of $\mathcal{N}(A) \subset E(V)$. Suppose A^* is ∂ -compressible in $E(V_0)$, and D is a ∂ -compressing disk. Then, since 5_1 is irreducible, $E(V_0)$ is ∂ -irreducible. Therefore compressing A^* along D yields an inessential disk in $E(V_0)$. This, along with the incompressibility of A^* , shows that A^* is ∂ -parallel to an annulus A^{**} in ∂V_0 . Since A^* is essential in E(V), A^{**} meets A_+ or A_- . Since ∂A^* is disjoint from $A_+ \cup A_-$, A^{**} contains either both A_+, A_- or one of



(a) 7_{40} and annulus A.



(b) 7_{41} and annulus A'.



(c) 5_1 and annulus A_0 .

Figure 6.2

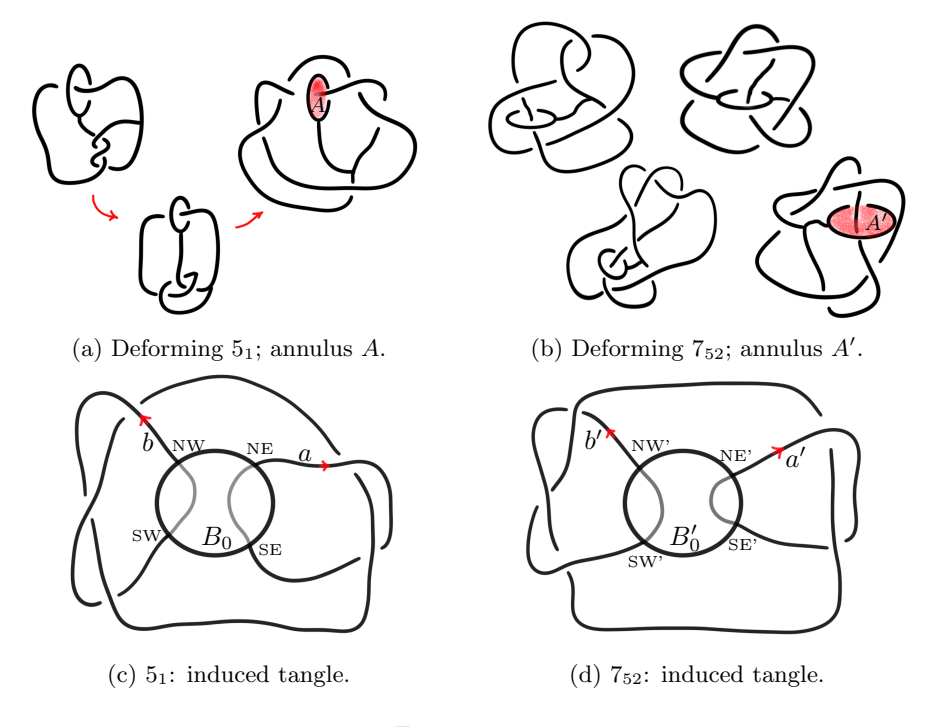


Figure 6.3

them. The former is impossible since the cores of A_+ , A_- are non-parallel in ∂V_0 , whereas the latter contradicts that A^* is not isotopic to A.

As a result, $A^* \subset E(V_0)$ is ∂ -incompressible and hence essential, but this contradicts that A_0 is the unique essential annulus in $E(V_0)$ and ∂A_0 meets $A_+ \cup A_-$. The same argument applies to V'.

Suppose 7_{40} , 7_{41} are equivalent, up to mirror image, and $f: (\mathbb{S}^3, V) \to (\mathbb{S}^3, V')$ is a homeomorphism. Then by the uniqueness of A, A', it may be assumed that f(A) = A' and hence f induces a self-homeomorphism of 5_1 that reverses the orientation of ∂A_0 , contradicting that every self-homeomorphism of 5_1 is isotopic to the identity by [17, Theorem 1.2].

Theorem 6.3. 5_1 and 7_{52} are inequivalent.

Proof. Denote by V, V' the handlebody-knots $5_1, 7_{52}$, respectively, and observe that E(V) (resp. E(V')) admits an essential annulus A (resp. A'); see Fig. 6.3a (resp. 6.3b). Since a component of ∂A (resp. $\partial A'$) bounds a non-separating disk D in V (resp. D' in V'), $A \subset E(V)$ (resp. $A' \subset E(V')$) is the unique essential annulus by [18, Theorem 1.4].

Suppose 5_1 and 7_{52} are equivalent, up to mirror image, and $f:(\mathbb{S}^3,V)\to(\mathbb{S}^3,V')$ is a homeomorphism. Then it may be assumed that f(A)=A', and hence f induces a self-homeomorphism g of \mathbb{S}^3 sending $V_A:=V\cup\mathcal{N}(A)$ to $V_A':=V'\cup\mathcal{N}(A')$. Let A_a,A_b (resp. A_a',A_b') be the two annuli in the frontier of $\mathcal{N}(A)\subset E(V)$ (resp. $\mathcal{N}(A')\subset E(V')$). Then the cores of A_a,A_b (resp. A_a',A_b') bound two disks in V_A (resp. V_A'). Denote by $a,b\subset V_A$ (resp. $a',b'\subset V_A'$) the arcs dual to the two disks, respectively. Also, orient the arcs a,b (resp. a',b') so they point away from D (resp. D'); see Fig. 6.3c (resp. 6.3d). In particular, the union $a\cup b$ (resp. $a'\cup b'$) can be regarded as a 2-string tangle in the exterior B of a regular neighborhood B_0 of $A\cup D$ (resp. the exterior B' of a regular neighborhood B'_0 of $A'\cup D'$).

Let NW,NE,SW,SE (resp. NW',NE',SW',SE') be the four boundary points of $a \cup b$ (resp. $a' \cup b'$) as shown in Fig. 6.3c (resp. 6.3d). Then g restricts to a homeomorphism from B_0 to B'_0 carrying XX to XX', where XX=NW,NE,SW or SE. Consider a ∞ -rational tangle t in B_0 ; see Fig. 6.3c. Then g(t) = t' is a $\frac{p}{q}$ -rational tangle in B'_0 , where q is necessarily even since NE' and SE' are joined by a string. If $p \neq 0$, then g gives an equivalence between a Montesions link and a composite link, contradicting that Montesions links are prime. As a result, (B'_0, t'_0) is also an ∞ -rational tangle, and hence g induces an equivalence between two oriented links $L := a \cup b \cup t_0$, $L' := a' \cup b' \cup t'_0$. Since L (resp. L') is a composition of a right-hand (resp. left-hand) trefoil and the Hopf link, g is orientation-reserving, contradicting that the linking numbers of both L and L' are 1.

Acknowledgements

The first author is member of the GNAMPA-INdAM. The forth author gratefully acknowledges the support from NSTC, Taiwan (grant no. 112-2115-M-110 -001 - MY3).

References

- [1] G. Bellettini, M. Paolini, Y.-S. Wang, A complete invariant for connected surfaces in the 3-sphere, J. Knot Theory Ramifications 29 (2020), 1–24.
- [2] G. Bellettini, M. Paolini, Y.-S. Wang, Numerical irreducibility criteria for handlebody links, Topology Appl. 284 (2020), 1–14.
- [3] G. Bellettini, M. Paolini, Y.-S. Wang, Unique 3-decomposition and mapping classes of knotted handlebodies, Geom. Dedicata 219(74) (2025).
- [4] G. Bellettini, G. Paolini, M. Paolini, Y.-S. Wang, A table of n-component handlebody links of genus n + 1 up to six crossings, Math. Proc. Camb. Phil. Soc. 174 (2023), 199–223.
- [5] G. Bellettini, G. Paolini, M. Paolini, Y.-S. Wang, Effects of tangle replacement on neighborhood equivalence classes, arXiv:2511.07796.
- [6] S. Buoncristiano, Fragments of Geometric Topology from the Sixties, Geometry and topology monographs 6, University of Warwick, Mathematics Institute (2003).
- [7] A. Ishii, Moves and invariants for knotted handlebodies, Algebr. Geom. Topol. 8 (2008), 1403–1418.
- [8] A. Ishii, K. Kishimoto, H. Moriuchi, M. Suzuki, A table of genus two handlebody-knots up to six crossings, J. Knot Theory Ramifications 21 (2012), 1250035 (9 pages).
- A. Ishii, K. Kishimoto, M. Ozawa, Knotted handle decomposing spheres for handlebody-knots,
 J. Math. Soc. Japan 67 (2015), 407–417.
- [10] J. H. Lee, S. Lee, Inequivalent handlebody-knots with homeomorphic complements, Algebr. Geom. Topol. 12 (2012), 1059—1079.
- [11] H. Moriuchi, An enumeration of theta-curves with up to seven crossings, J. Knot Theory Ramifications 18 (2009), 67–197.
- [12] H. Moriuchi, A table of handcuff graphs with up to seven crossings, OCAMI Studies Vol 1. Knot Theory for Scientific objects (2007) 179–300.
- [13] H. Moriuchi, A table of θ-curves and handcuff graphs with up to seven crossings, Adv. Stud. Pure Math. Noncommutativity and Singularities: Proceedings of French–Japanese symposia held at IHES in 2006, J.-P. Bourguignon, M. Kotani, Y. Maeda and N. Tose, eds. (Tokyo: Mathematical Society of Japan, 2009), 281–290.
- [14] M. Motto, Inequivalent genus two handlebodies in S³ with homeomorphic complements, Topology Appl. 36(3) (1990), 283–290
- [15] M. Paolini, Appcontour. Computer software. Vers. 2.5.8. Apparent contour. (2018) <git@github.com:appcontour/appcontour.git/>.
- [16] M. Paolini (2024, July 24). Complete table of handlebody knots of genus 2 up to seven crossings. http://dmf.unicatt.it/paolini/handlebodies/
- [17] Y.-S. Wang, Unknotting annuli and handlebody-knot symmetry, Topol. Appl. 305(1) (2022), 107884.
- [18] Y.-S. Wang, JSJ decomposition for handlebody-knots, J. Math. Soc. Japan 76(4) (2024), 1049–1085.
- [19] H. Whitney, Congruent graphs and the connectivity of graphs, Am. J. Math. 54 (1932), 150–168.
- [20] E. C. Zeeman, Seminar on combinatorial topology, Notes I.H.E.S. and Warwick (1963).

DIPARTIMENTO DI SCIENZE MATEMATICHE, INFORMATICHE E FISICHE, VIA DELLE SCIENZE 206, 33100 Udine UD, Italy and International Centre for Theoretical Physics ICTP, Mathematics Section, 34151 Trieste, Italy

 $Email\ address: {\tt giovanni.bellettiniQuniud.it}$

Dipartimento di Matematica, Università di Bologna, Piazza di Porta San Donato 5, 40126 Bologna, Italy

 $Email\ address{:}\ {\tt g.paolini@unibo.it}$

Dipartimento di Matematica e Fisica, Università Cattolica del Sacro Cuore, 25121 Brescia, Italy

 $Email\ address: \verb|maurizio.paolini@unicatt.it|$

NATIONAL SUN YAT-SEN UNIVERSITY, KAOHSIUNG, TAIWAN

 $Email\ address{:}\ {\tt yisheng@math.nsysu.edu.tw}$